E-MRS 2022 Fall Meeting

19th - 22nd September 2022

Free-standing InSb nanostructures: growth, morphology control and electrical characterization

Valentina Zannier[1], Isha Verma[1], Sedighe Salimian[1], Stefan Heun[1] , Francesca Rossi[2], Daniele Ercolani[1], Fabio Beltram[1], and Lucia Sorba[1]

[1] NEST-Istituto Nanoscienze CNR-Scuola Normale Superiore di Pisa, Italy

[2] IMEM-CNR, Parma, Italy

valentina.zannier@nano.cnr.it

Outline

- **InSb nanostructures**: motivation and challenges
- **InSb morphology control** on InAs nanowire stems: nanowires (1D), nanoflags (2D), nanocubes (3D)
- **Directional growth**: results and modelling
- **InSb nanoflags**: structural and electrical properties

Motivation

InSb:

- Small bandgap, low electron effective mass, high electron mobility, high Landè g-factor and strong spin-orbit interaction
  → promising material for optoelectronics, thermoelectrics, spintronics and quantum computing

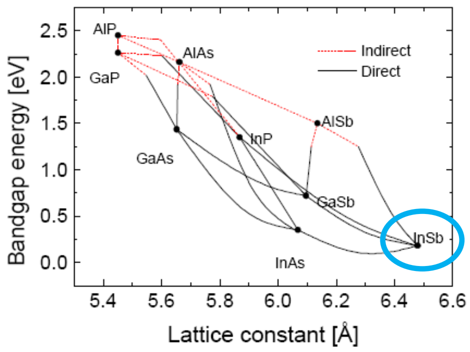

- Large lattice mismatch with all other III-Vs → difficult integration of defect-free InSb in planar epitaxy
- Sb acts as a surfactant → difficult to control/tune the InSb morphology during the growth

Free-standing InSb nanostructures:

- ✓ Defect-free growth of heterostructures
- ✓ High surface/volume ratio
- ✓ Carriers confinement

Heteroepitaxy: bulk crystal vs nanostructures

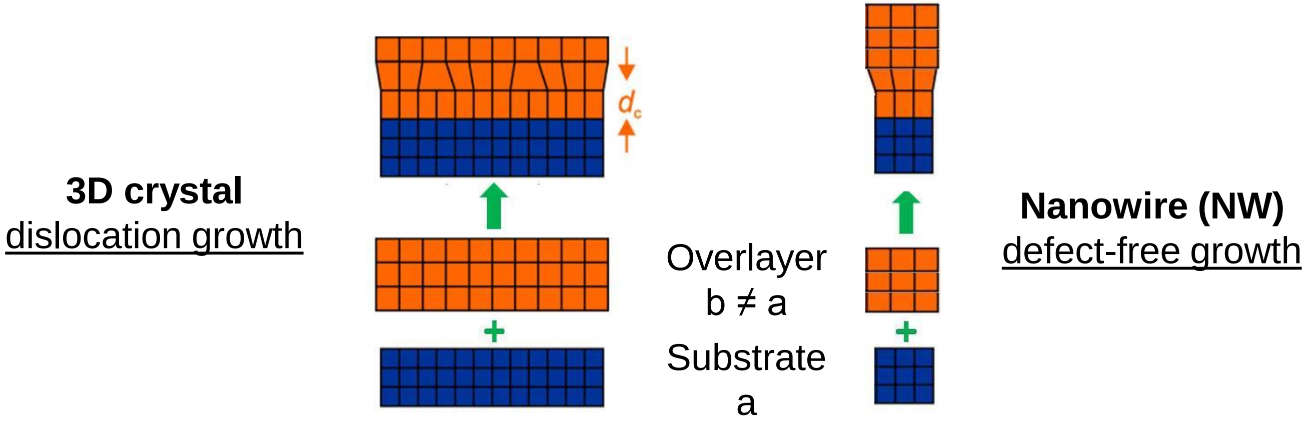

Motivation

Free-standing InSb nanostructures (1D)

InSb heterostructure nanowires: MOVPE growth under extreme lattice mismatch

Philippe Caroff[1], Maria E Messing, B Mattias Borg, Kimberly A Dick, Knut Deppert and Lars-Erik Wernersson

Nanotechnology 20 (2009) 495606

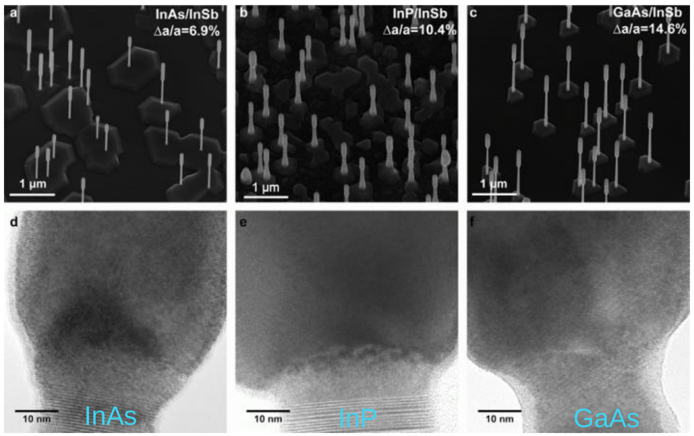

InAs/InSb nanowire heterostructures grown by chemical beam epitaxy

Daniele Ercolani[1], Francesca Rossi[2], Ang Li[3], Stefano Roddaro[1], Vincenzo Grillo[3], Giancarlo Salviati[2], Fabio Beltram[1] and Lucia Sorba[1]

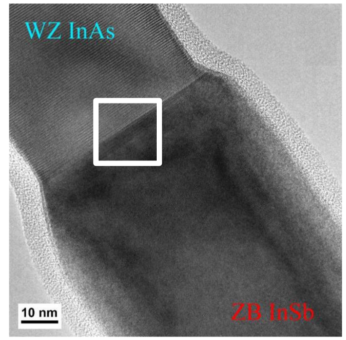

Nanotechnology 20 (2009) 505605

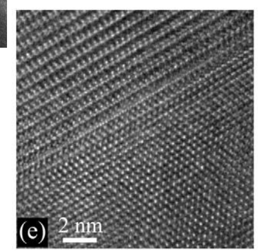

Hard Superconducting Gap in InSb Nanowires

Önder Gül, Hao Zhang, Folkert K. de Vries, Jasper van Veen, Kun Zuo, Vincent Mourik, Sonia Conesa-Boj, Michał P. Nowak, David J. van Woerkom, Marina Quintero-Pérez, Maja C. Cassidy, Attila Geresdi, Sebastian Koelling, Diana Car, Sébastien R. Plissard, Erik P. A. M. Bakkers, and Leo P. Kouwenhoven

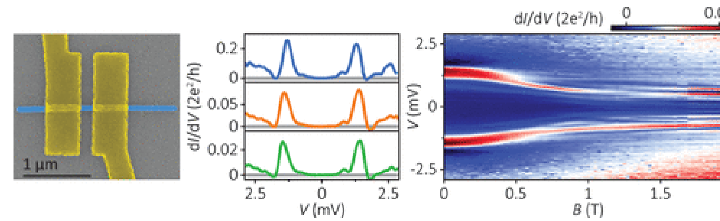

Nano Lett. 17 (2017), 4, 2690–2696

(2D)

Twin-Induced InSb Nanosails: A Convenient High Mobility Quantum System

María de la Mata, Renaud Leturcq, Sébastien R. Plissard, Chloé Rolland, César Magén, Jordi Arbiol, and Philippe Caroff

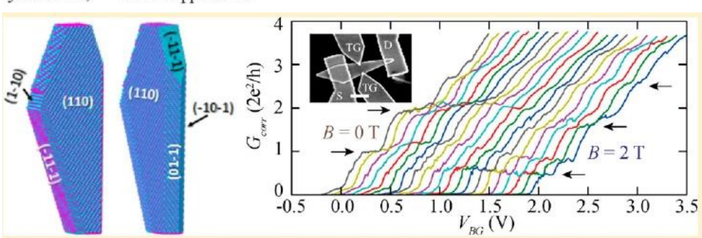

Nano Lett. 16 (2016) 825

Free-Standing Two-Dimensional Single-Crystalline InSb Nanosheets

D. Pan, D. X. Fan, N. Kang, J. H. Zhi, X. Z. Yu, H. Q. Xu, and J. H. Zhao

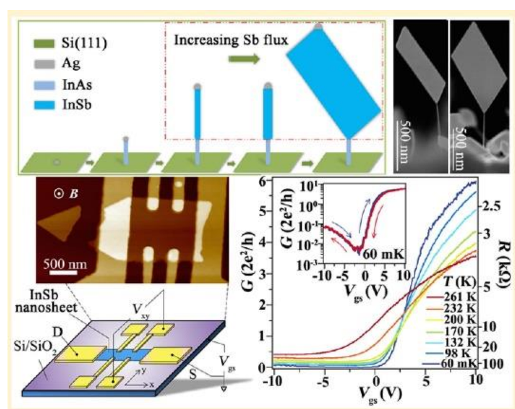

Nano Lett. 16 (2016) 834

Bottom-Up Grown 2D InSb Nanostructures

Sasa Gazibegovic, Ghada Badawy,* Thijs L. J. Buckers, Philipp Leubner, Jie Shen, Folkert K. de Vries, Sebastian Koelling, Leo P. Kouwenhoven, Marcel A. Verheijen, and Erik P. A. M. Bakkers*

Adv. Mater. 31 (2019) 1808181

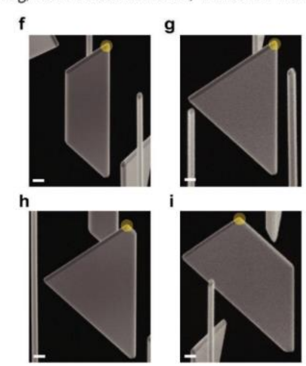

Our approach

OUR GOALS: - **morphology control** of **high quality InSb nanostructures** by tuning the growth parameters
- develop a directional **growth protocol** to achieve **free standing InSb nanoflags** on NW stems

OUR APPROACH: <u>Au assisted Chemical Beam Epitaxy</u> using Au nanoparticle from colloidal solutions

Chemical Beam Epitaxy (CBE)

Ultra High Vacuum (UHV) chamber

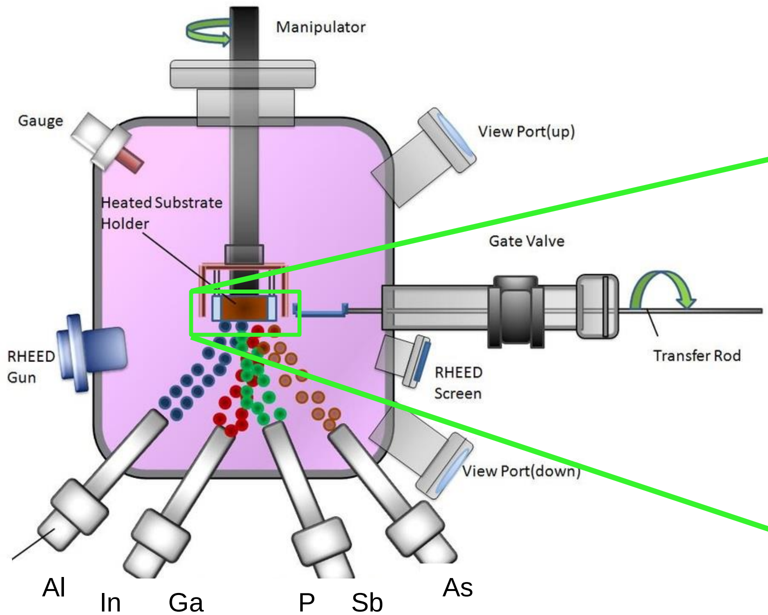

Nanoparticle (NP) assisted vapour-liquid-solid (**VLS**) mechanism

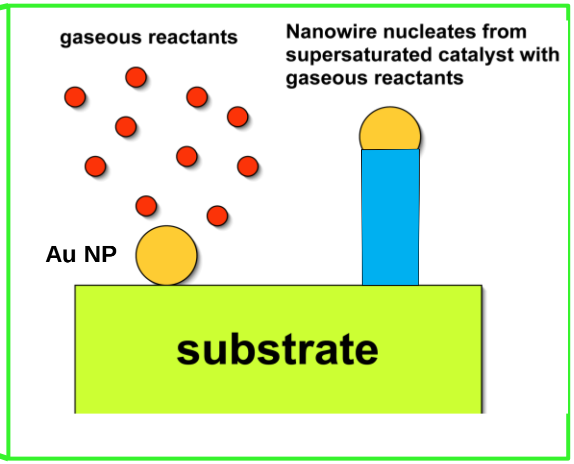

VLS growth occurs when a liquid alloy droplet starting from a metal nanoparticle (NP) becomes supersaturated with material from a gaseous reactant. The material then precipitates from the solid-liquid interface to form a nanowire.

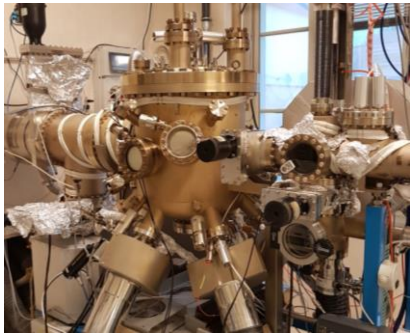

CBE at NEST: Riber Compact-21 CBE system
Metal-organic precursors:
Group III : TM**In**, TE**Ga**, TM**Al**
Group V : TB**As**, TB**P**, TDMA**Sb**, TM**Sb**
n-doping: TB**Se**

Morphology control of InSb nanostructures

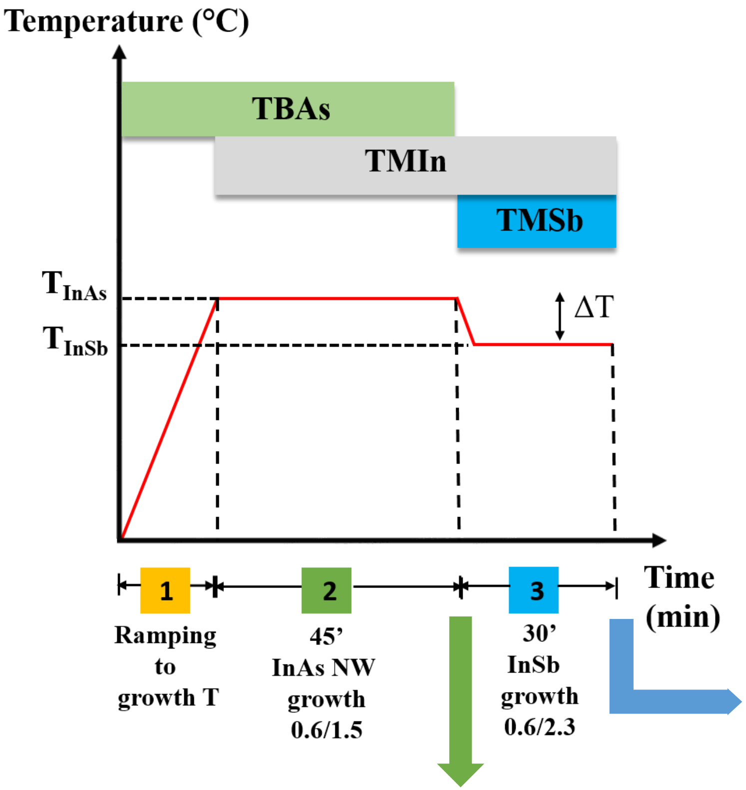

Substrates: InAs (111)B, Au nanoparticles: 30 nm colloids
MO precursors: TBAs, TMIn, TMSb. Sample rotation: 5 rpm

InSb growth: T optimization

ΔT = -20°C **ΔT = -30°C** **ΔT = -40°C**

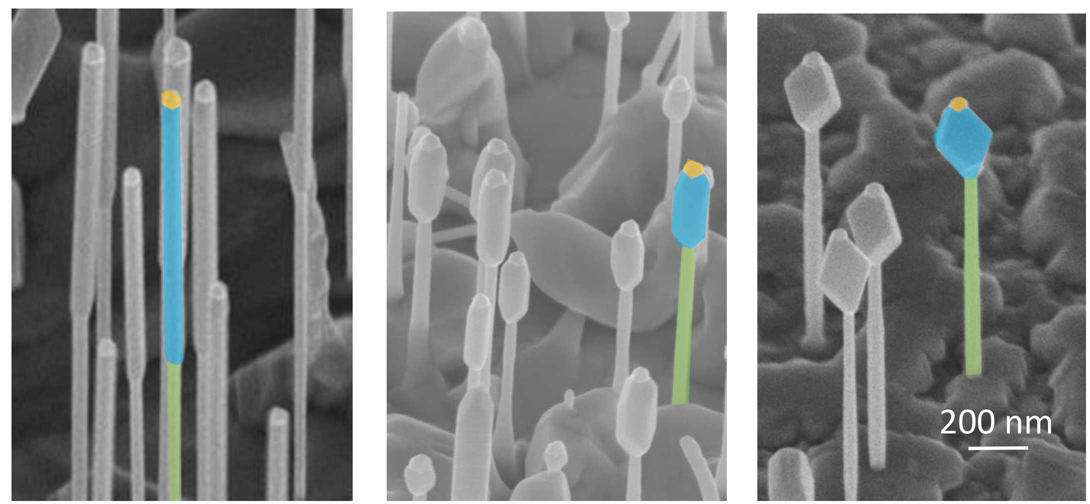

1D- like Nanowires

3D- like Nanocubes

InAs nanowire stems

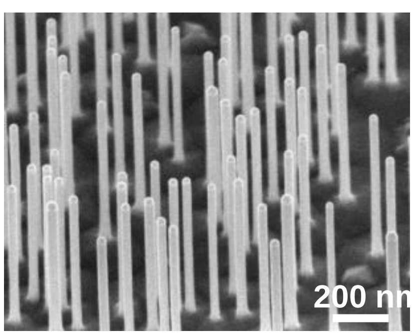

T_{InAs} : 385°C

Low T enhances the radial growth and reduces the axial growth

InSb nanowires

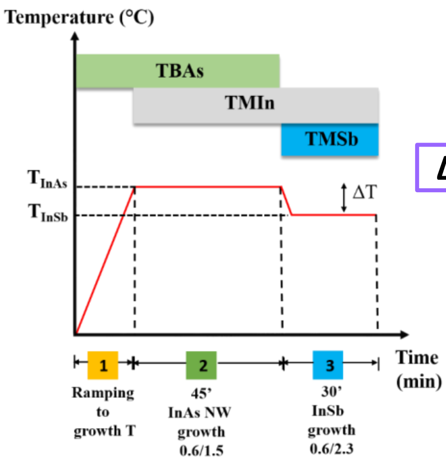

ΔT = -20°C

With sample rotation uniform InSb growth

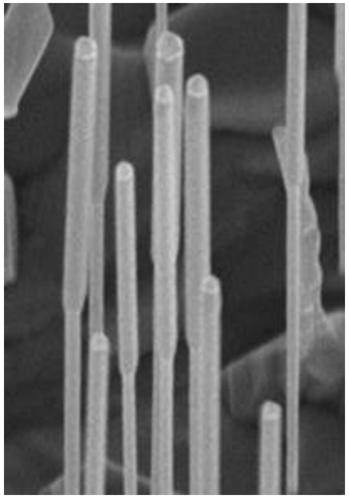

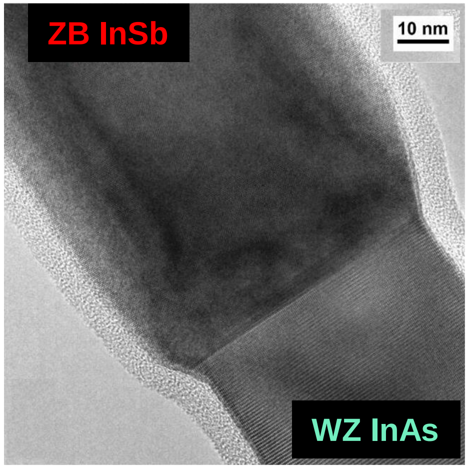

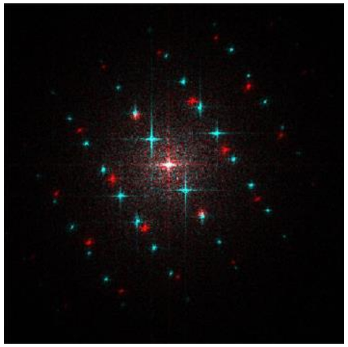

InSb: <110> zone axis
InAs: <2-1-10> zone axis

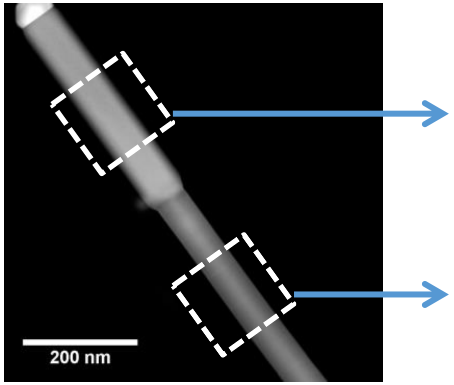

HAADF profile

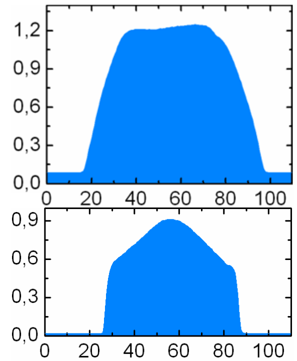

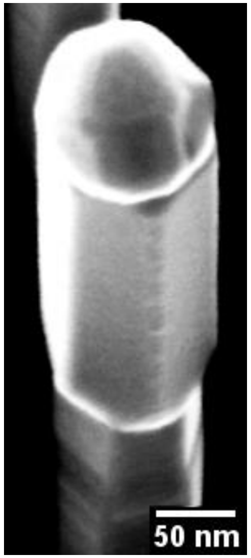

Top-view: NW cross-section

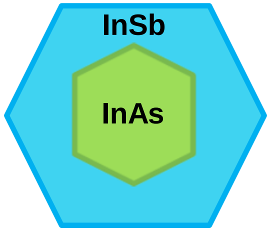

- **InAs NWs have WZ crystal structure with 6 equivalent {112} sidewalls**
- **InSb has ZB crystal structure with 6 equivalent {110} sidewalls**

D. Ercolani el al. *Nanotechnology* 20, 505605 (2009)
L. Lugani el al. *Cryst. Growth Des.*, 10, 4038 (2010)

Directional InSb radial growth

Sample alignment before InSb growth:

Top view

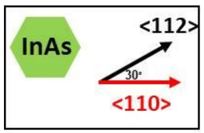

RHEED pattern
of InAs NW
in <110> direction

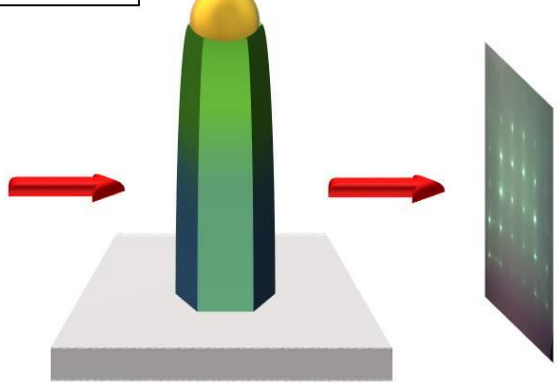

Side view

InSb growth at ΔT -30°C with NO sample rotation:

Sb beam projection aligned to {110} direction

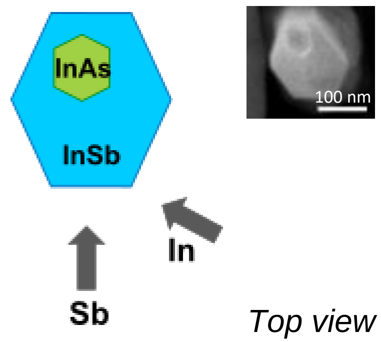

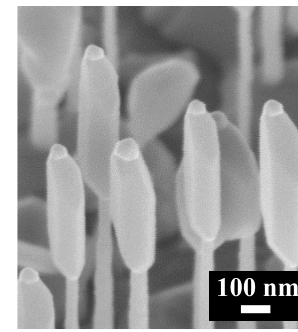

Top view *Side view*

Sb beam projection aligned to {112} direction

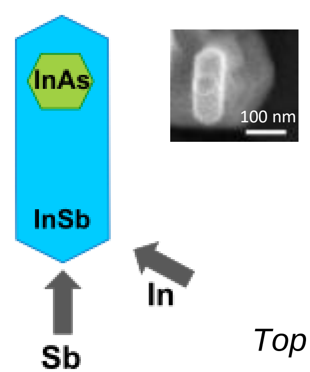

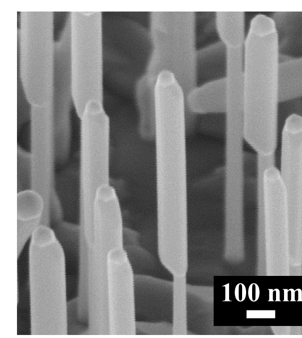

Top view *Side view*

Free-standing InSb nanoflags (NFs)

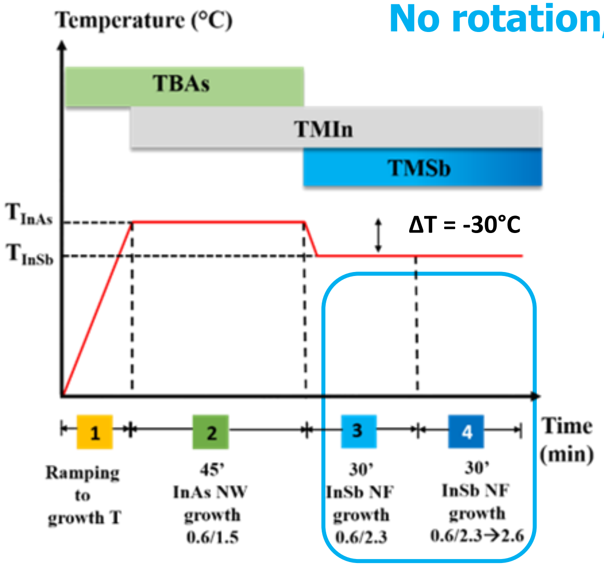

No rotation, alignment, increasing Sb flux → asymmetric growth enhancement

Top-view

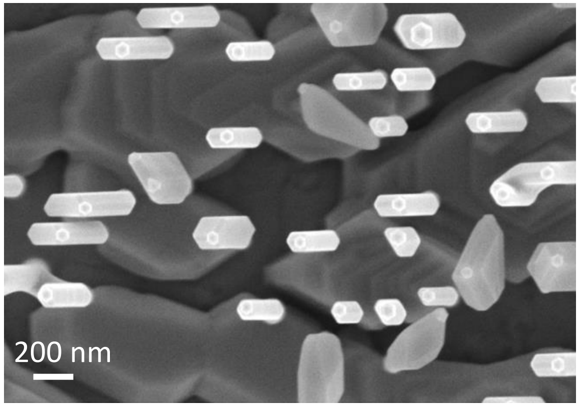

45°-tilted-view

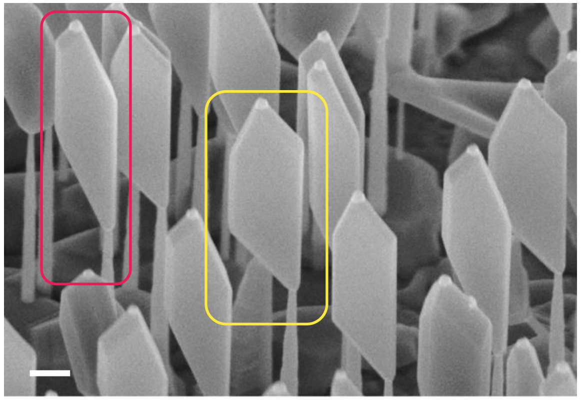

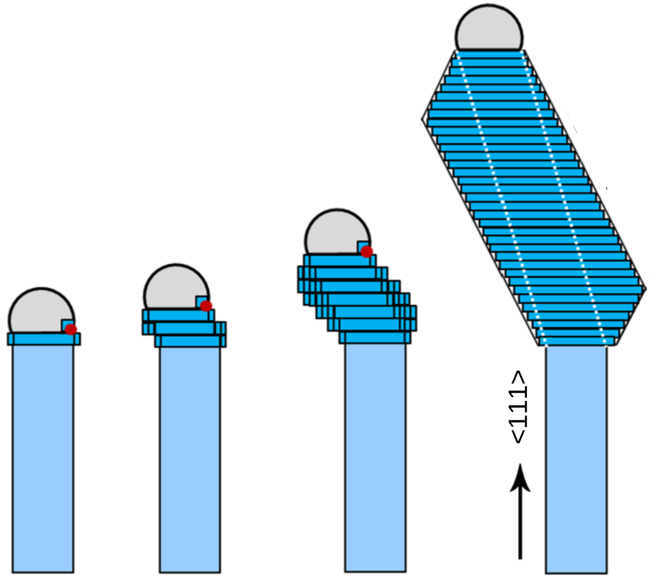

NF final shape is the result of the combined axial VLS growth and anisotropic radial growth, together with the mobility of the droplet (due to the high Sb flux), which crawls from left to right or right to left, along the direction of triple phase line.

2 different aperture angles: 145° and 160°

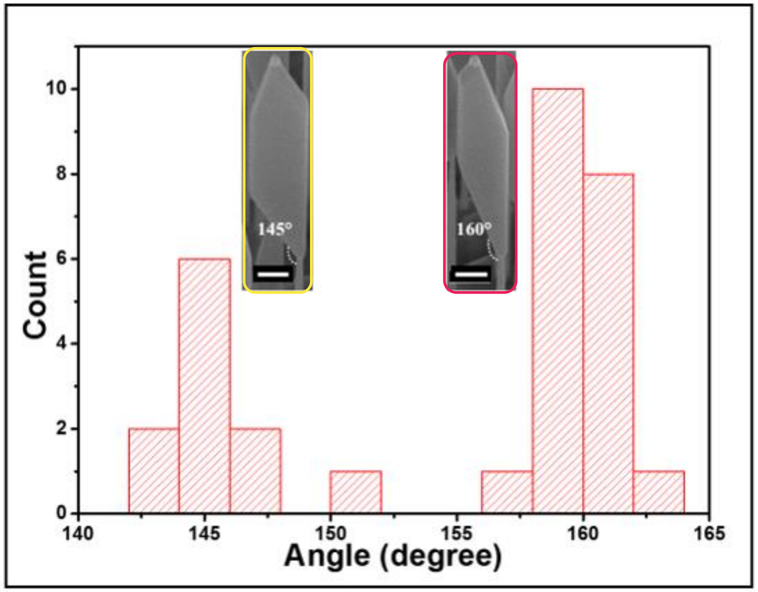

Nano Lett. 16 (2016) 834

Free-standing InSb nanoflags (NFs)

180° rotation around the growth axis of the additional facets at the interface

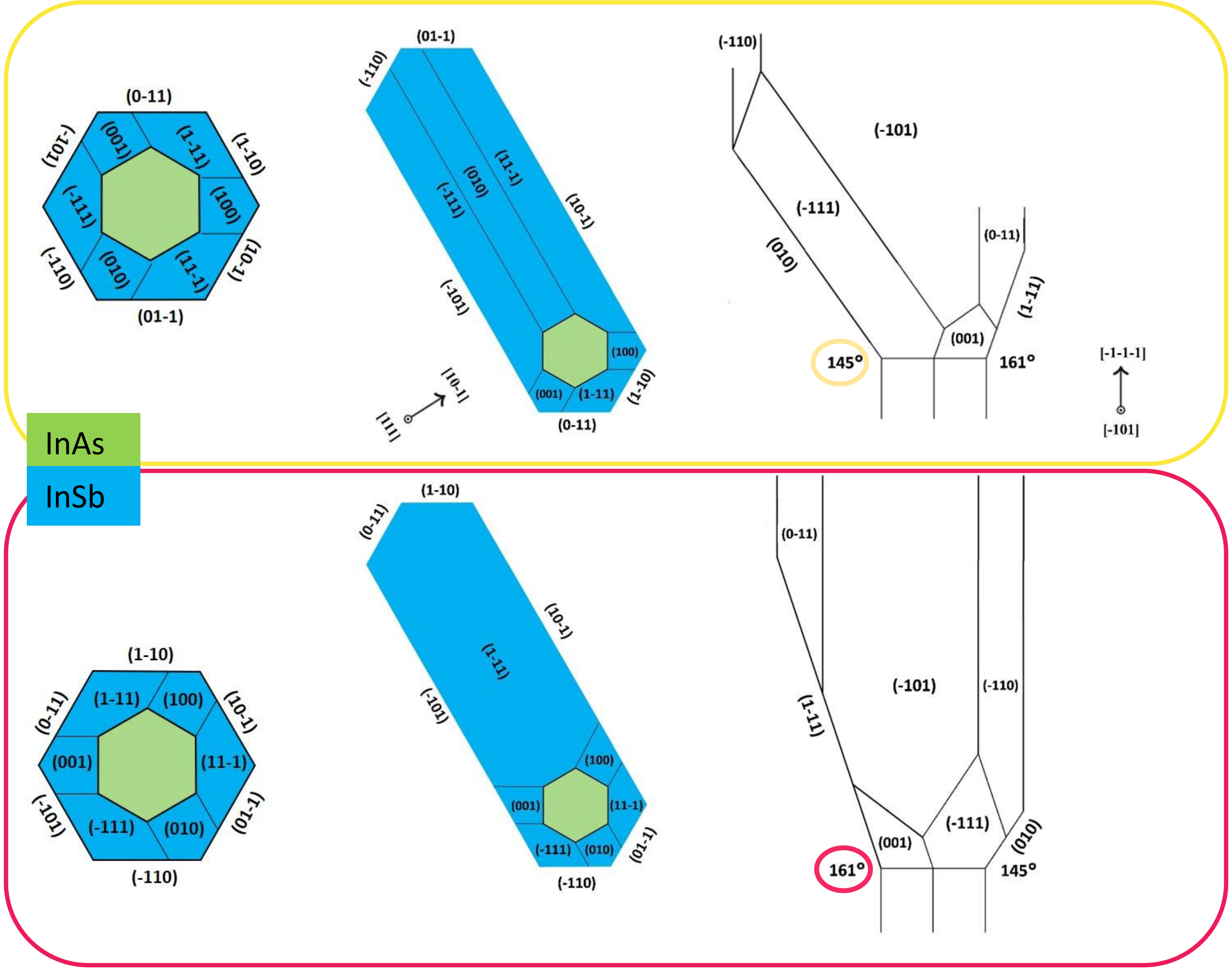

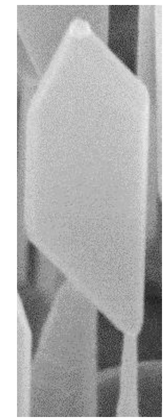

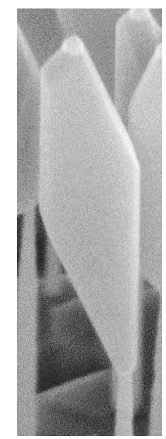

SYMMETRIC NW TOP VIEW

NANOFLAG TOP VIEW <111> projection

NANOFLAG SIDE VIEW <100> projection

Free-standing InSb nanoflags (NFs)

145° aperture angle

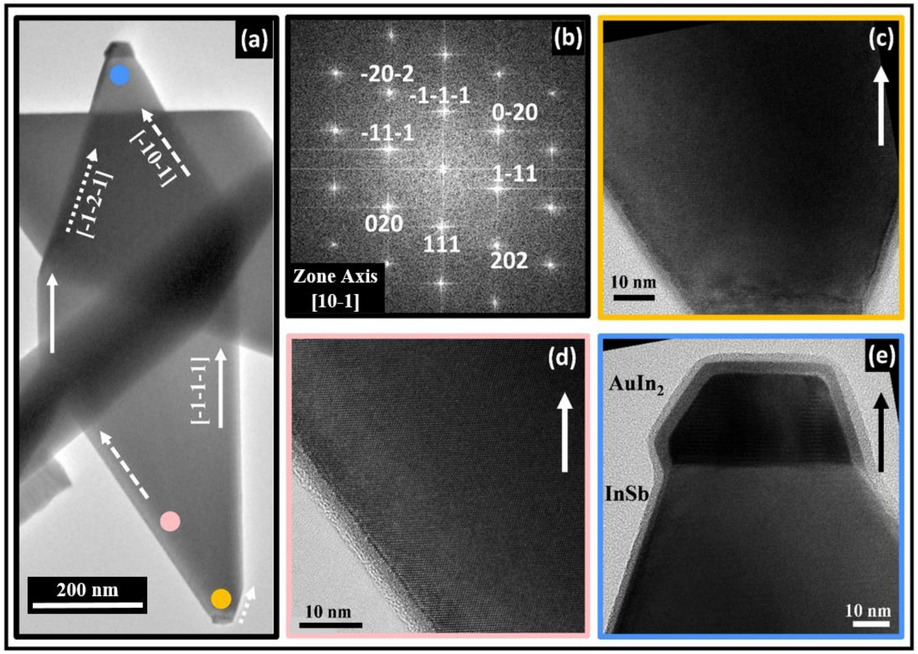

160° aperture angle

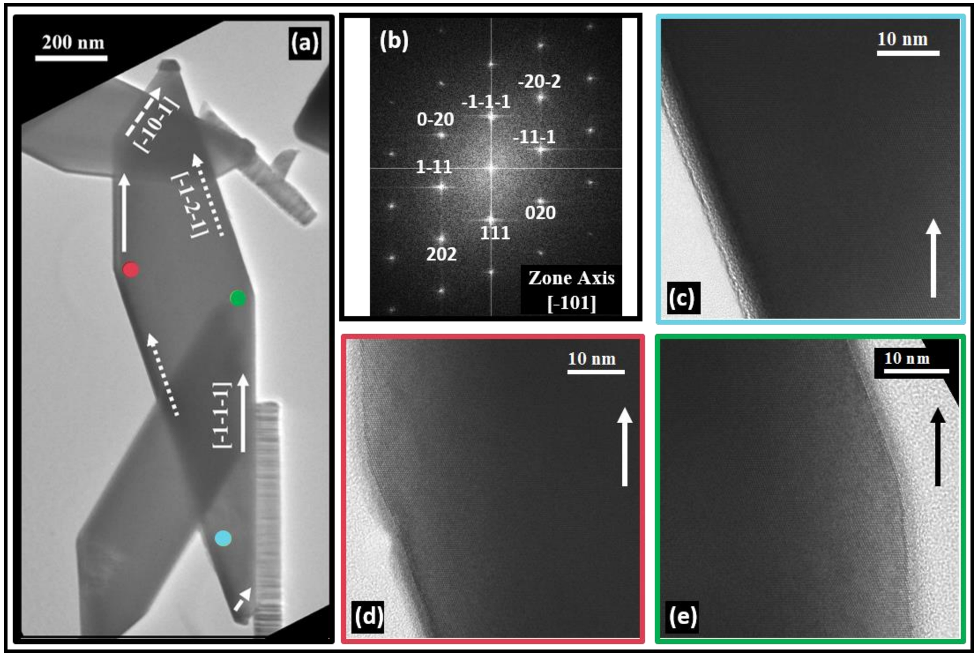

GPA

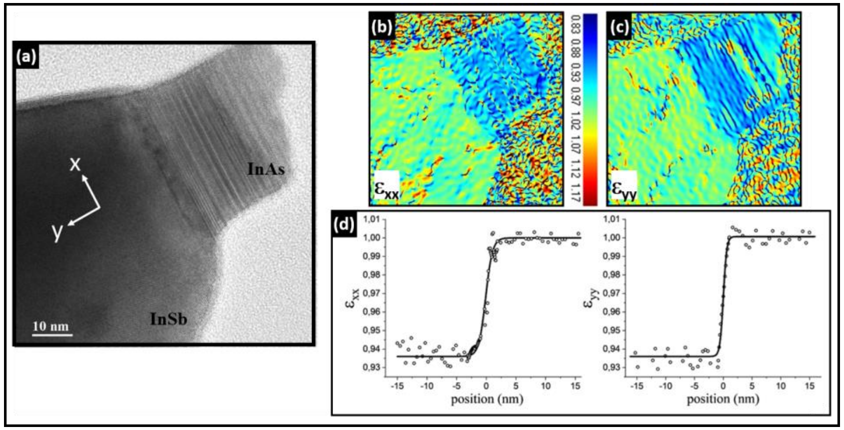

- Defect-free ZB crystal structure
- Stoichiometric composition
- Relaxed lattice parameter

- Still too small for practical use (multi-contact devices)

Verma *et al, Nanotechnology* **31** 384002 (2020)

Longer InSb growth time

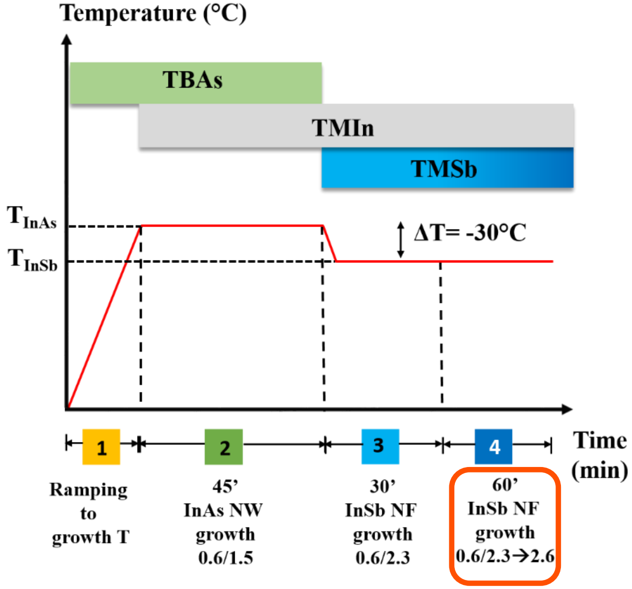

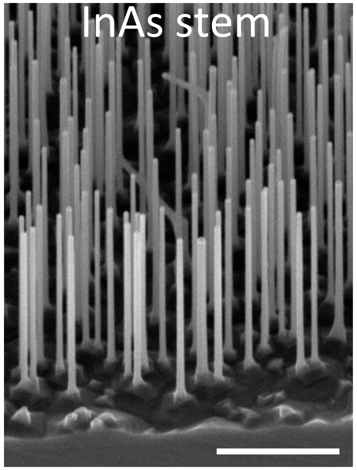

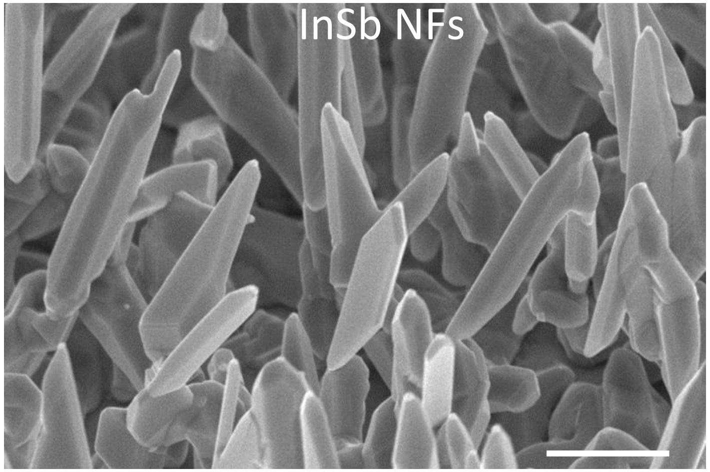

InAs stem bending and TMSb etcing

Increasing InSb growth time

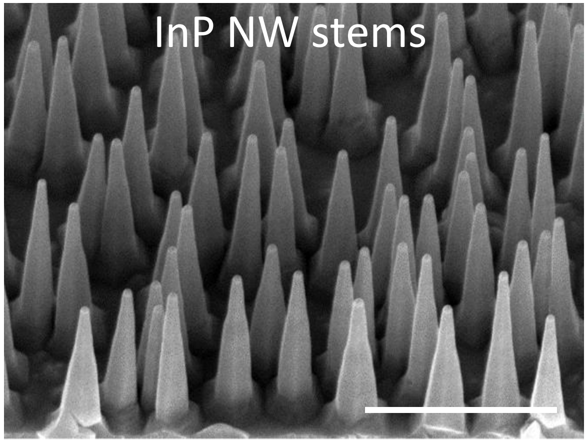

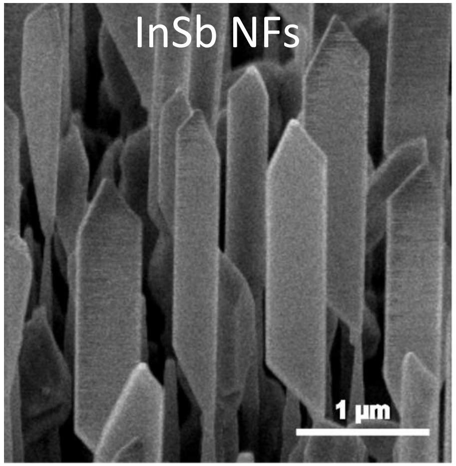

InSb NFs dimension
Length= 2.8 ± 0.2 µm
Width= 470 ± 80 nm
Thickness= 105 ± 20 nm

Using **tapered and more robust InP NW stems**, we could achieve bigger InSb NFs

Verma *et al, ACS Appl. Nano Mater* **4** 5825 (2021)

Larger InSb nanoflags

InP NWs have mixed WZ/ZB crystal structure, but still <112> sidewalls

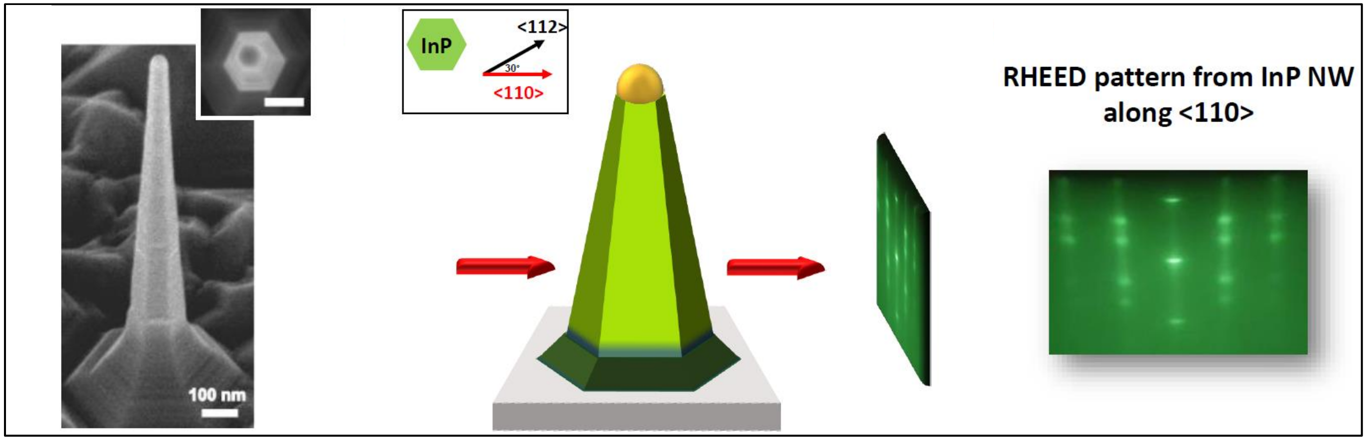

Sb beam projection aligned to {112} direction

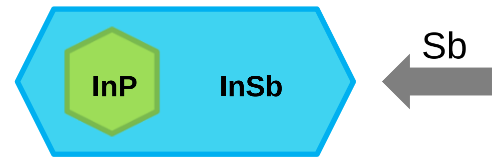

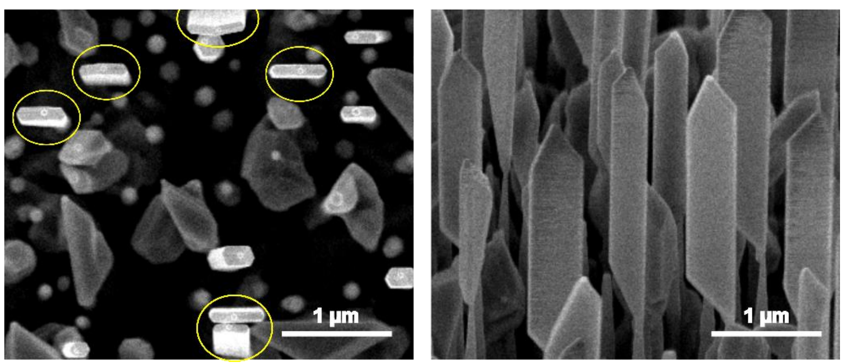

Lower yeld, but bigger NFs

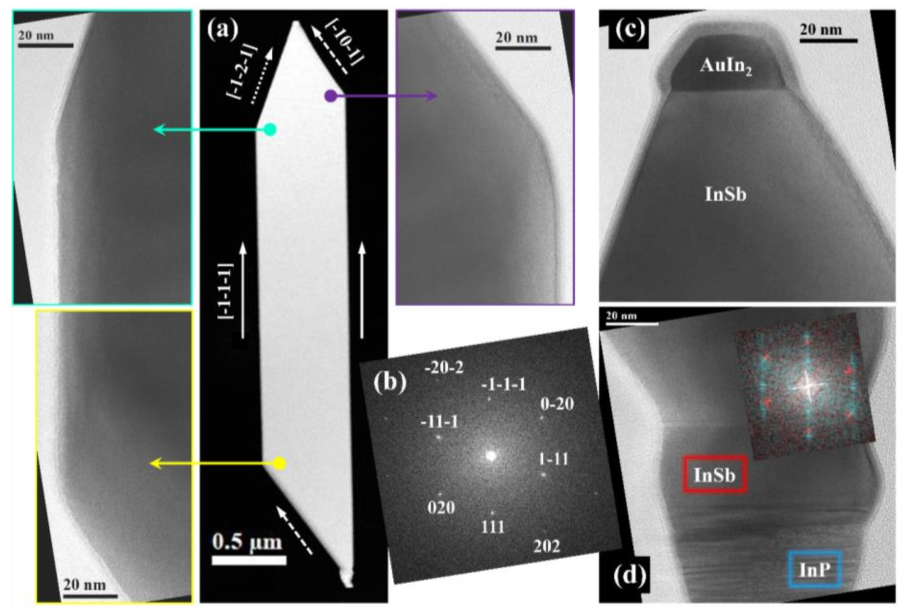

STEM-HAADF image and corresponding HRTEM images show **defect-free InSb ZB crystal structure**.

Morphological evolution of InSb NFs in regular arrays

Substrate preparation

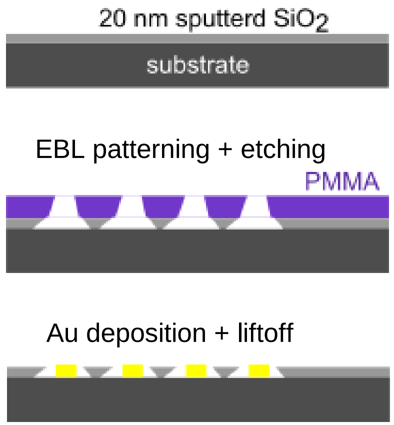

Top view SEM image

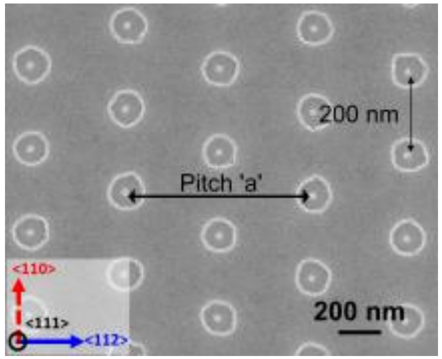

Pitch ‘a’: 500, 700, 900, 1100 and 1500 nm.

Selective area + VLS directional growth

InP nanowire stems

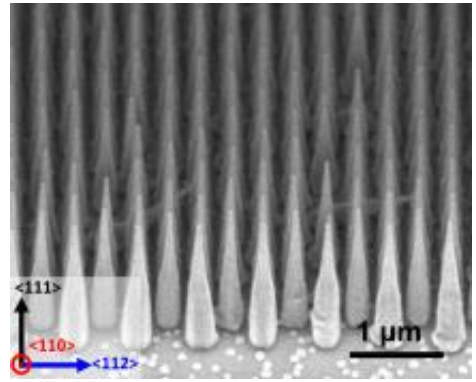

InSb nanoflags

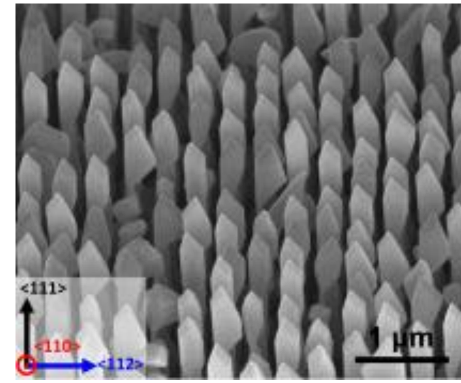

Pitch AND Sb projection in <112> direction

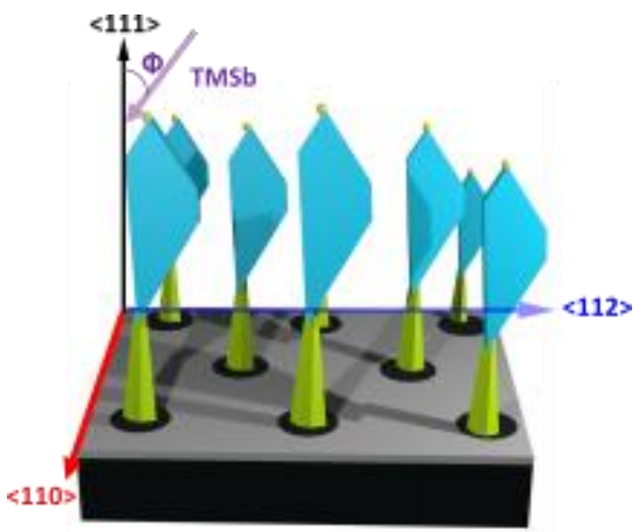

Measured geometrical parameters

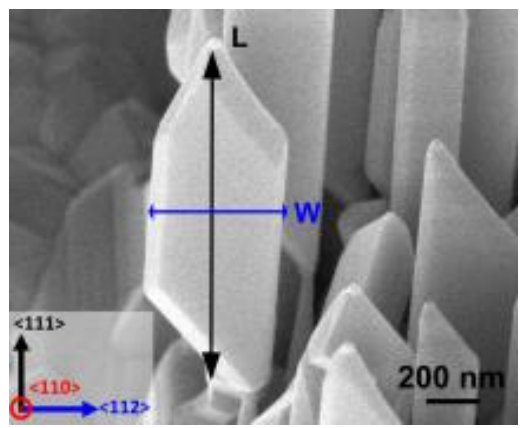

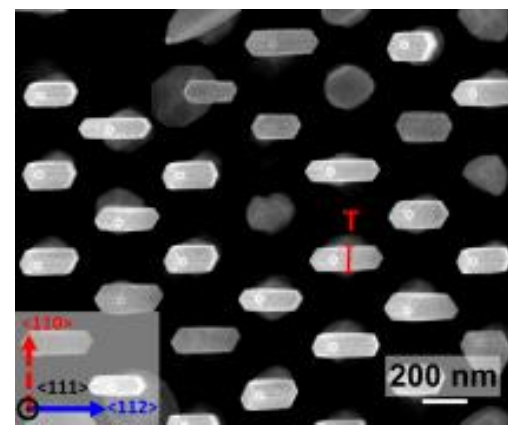

Thickness from top-view images
Length and Width from tilted images (45°)

Growth modelling

InSb NF length vs growth time for different pitches

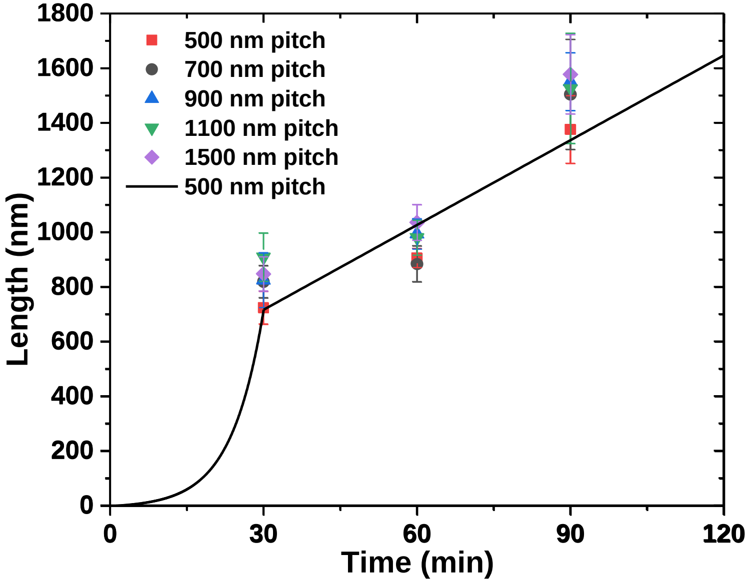

- Length evolution can be qualitatively explained by considering the **In-limited VLS axial growth** rate containing two contributions:
  (1) the direct impingement
  (2) In adatom diffusion on the sidewalls.
- Surface diffusion of In adatoms from the substrate can be neglected as InP NW is ~1.2 µm long.
- (1) is constant, (2) is higher at L< λ_{In}
  → For L> λ_{In} axial growth rate becomes constant

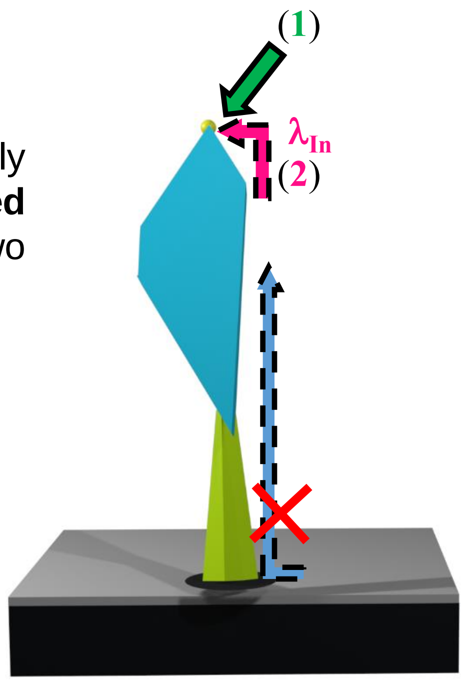

- Axial growth rate is higher at the beginning, then decreases.
- Lower axial growth rates for smaller pitches due to shadowing or competition
- For larger pitches (a ≥ 700 nm) the NF lengths are almost independent of the pitch, indicating no competition above this threshold.

Fitting is done for $\lambda_{In} = 724$ nm at $a = 500$ nm, with $A = 0.158$ min^{-1}, $B = 1$ nm/min, and $C = 0.013$ min^{-1}

SOLUTIONS

$$L = \frac{B}{A}(e^{At} - 1),\ L \leq \lambda_{In};$$
$$L = \lambda_{In} + (C\lambda_{In} + B)(t - t_0), L > \lambda_{In}$$

B describes direct impingement of In atoms onto catalyst surface.
A and C stand for the efficiencies of In adatom collection from the NW sidewalls (different in the 2 stages of the growth).
t_0 is the moment in time at which the NF length reaches λ_{In}.

Growth modelling

InSb NF width and thickness for different pitches

simplified 2D geometry (top-view)

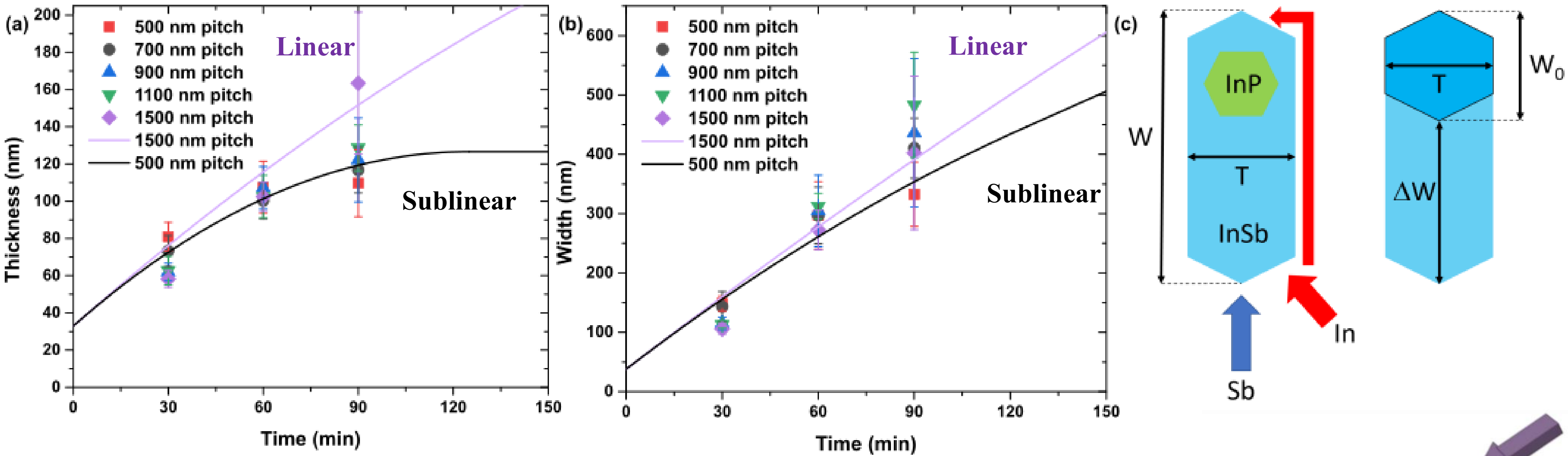

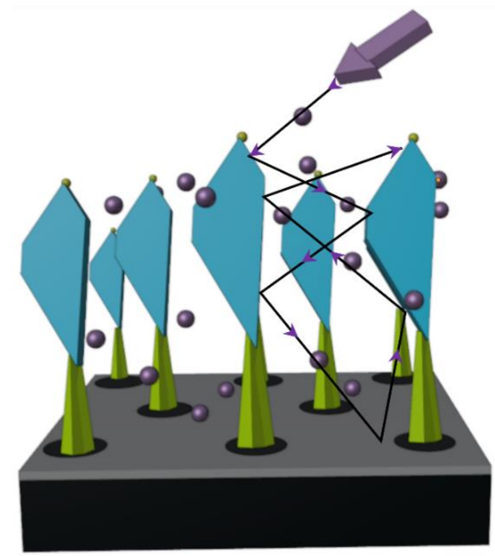

- Linear behavior for larger pitches. Sublinear for smaller pitches, T more than W.
- VS radial growth rate is Sb limited. If there were only direct Sb flux, T would be constant.
- We have to take into account **direct Sb flux** (directional) and **re-emitted Sb flux** (scattering of Sb atoms from NF sidewalls: non-directional, fully shadowed at smaller pitches)
- T increases only due to the re-emitted flux, while W has both contributions from re-emitted flux and from direct impingement of Sb flux on the 2 front facets (ΔW).
- W/T ratio can be increased by decreasing the pitch (shadowing suppresses re-emitted flux).

Thickness and width can be decoupled when re-emitted flux is completely suppressed!

NFs transport measurements

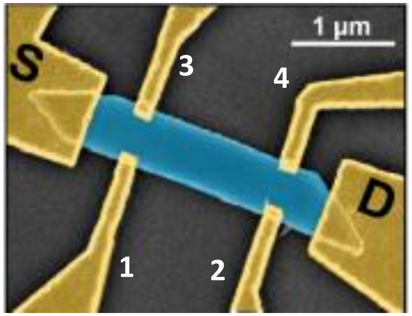

Hall-bar device

Channel width (width between contacts 1-3 and 2-4)=325 nm
Channel length (1-2 and 3-4)=1.5 µm. The NF thickness is ~100 nm.
Contacts: 10 nm Ti/190 nm Au
Substrate: Si/SiO_2

R_{SD}(RT, VBG=0 V) = 11 KΩ
R_{SD}(4.2K, VBG=50 V) = 2.5 KΩ

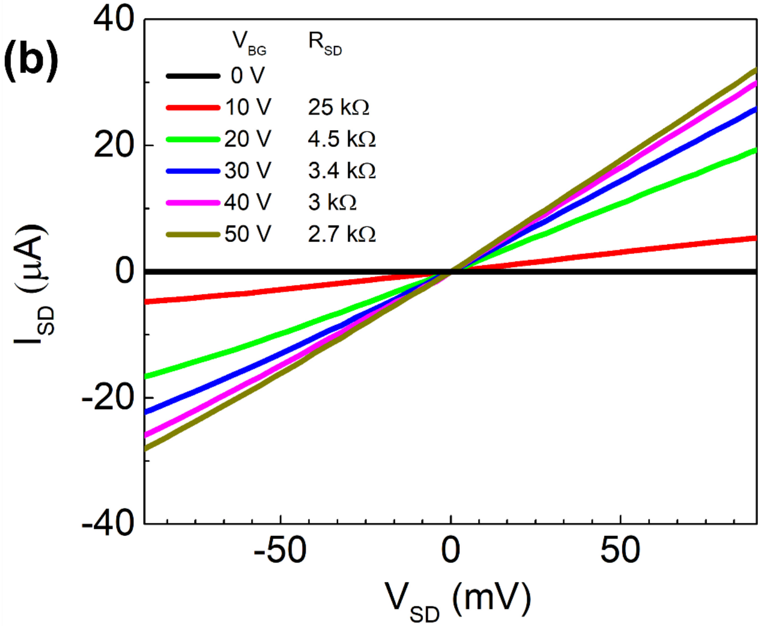

Source-drain current VS backgate voltage @ 4.2 K

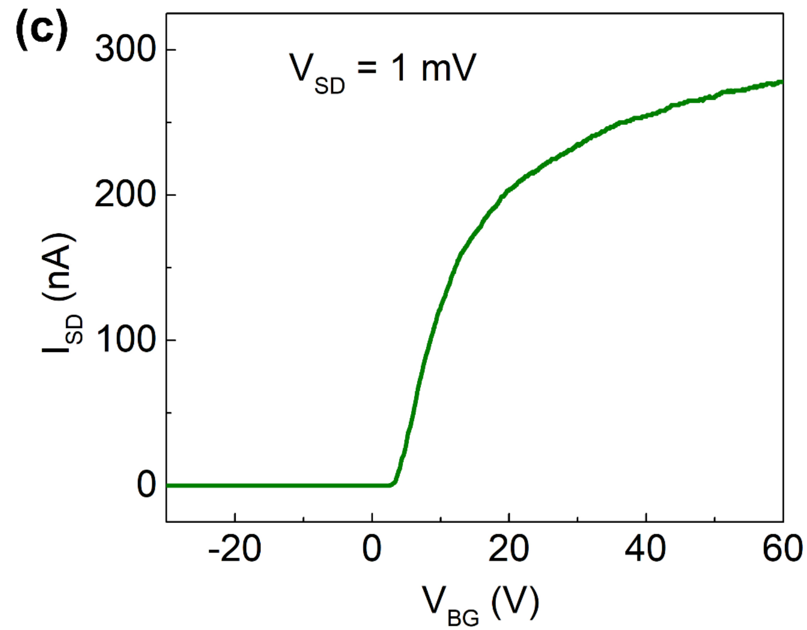

Good Ohmic contacts

n- type characteristics of InSb NFs under BG modulation

Field-effect mobility 28000 cm^2/Vs
from four-probe measurement (longitudinal voltage drop)

NFs transport measurements

Hall effect vs BG bias @ 4.2K

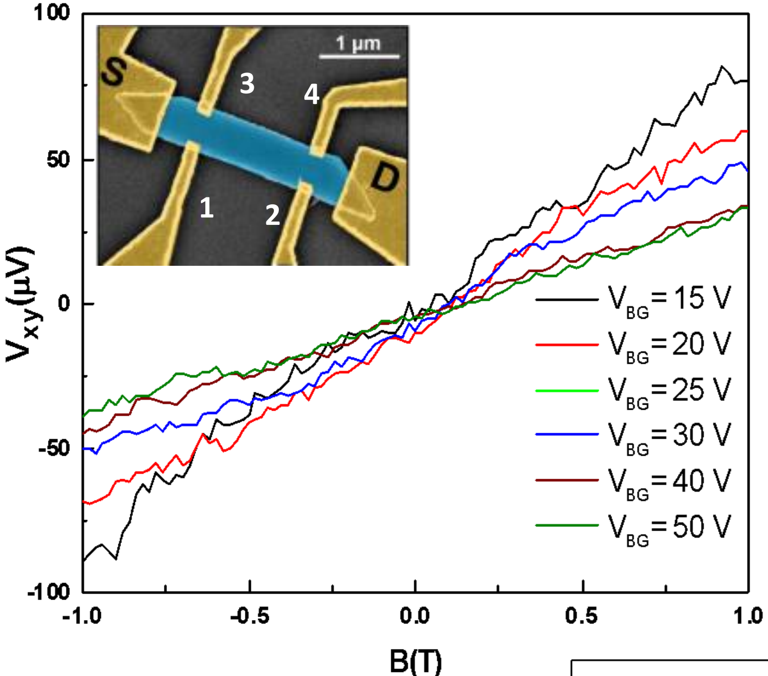

Electron Hall mobility = 29500 cm²/ Vs

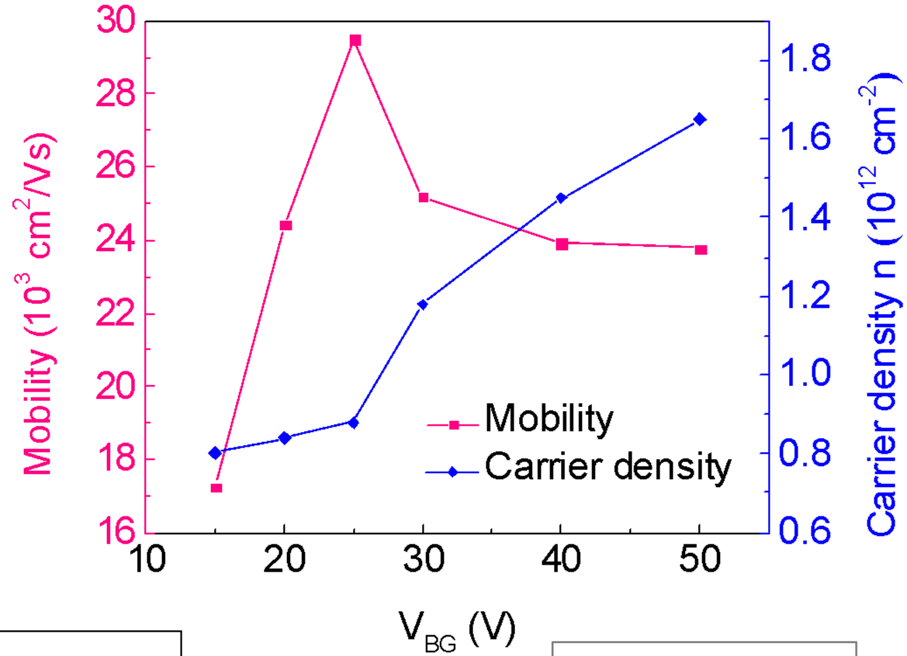

$$\mu_H = \frac{L}{W<V_{xx}>}\left(\frac{V_{xy}}{B}\right)$$

$$n = \frac{I}{e}\left(\frac{B}{V_{xy}}\right)$$

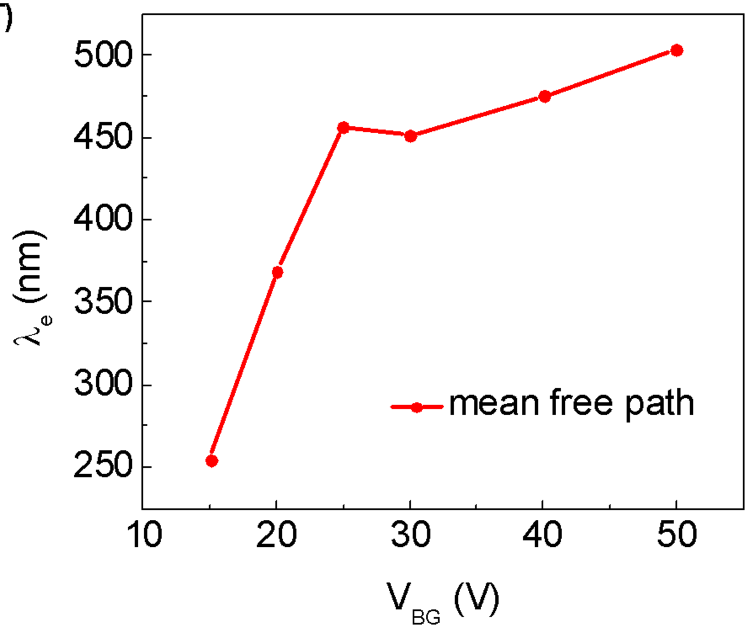

$\lambda_e = (\hbar\mu/e)(2\pi n)^{1/2}$

Mean free path λ_e up to 500 nm

Ballistic InSb NFs-based Josephson junction devices

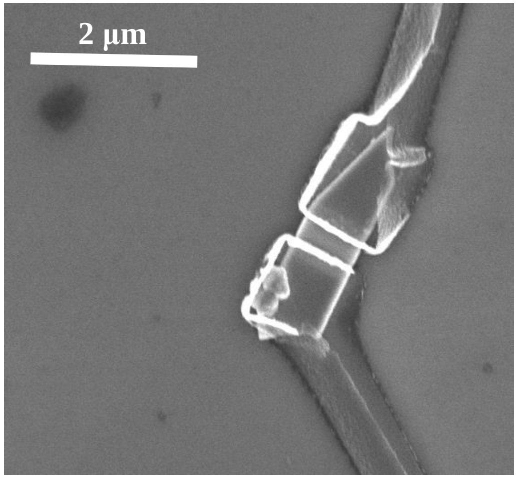

10 nm Ti/150 nm Nb
Substrate: Si/SiO_2

L = 200 nm
W = 700 nm
d = 100 nm

T_c = 8.44 K
$\Delta = 1.76\ k_B T_c = 1.28$ meV

Ballistic regime! Mean free path λ_e > length L of the junction, $\lambda_e > L$.

Voltage drop VS bias current

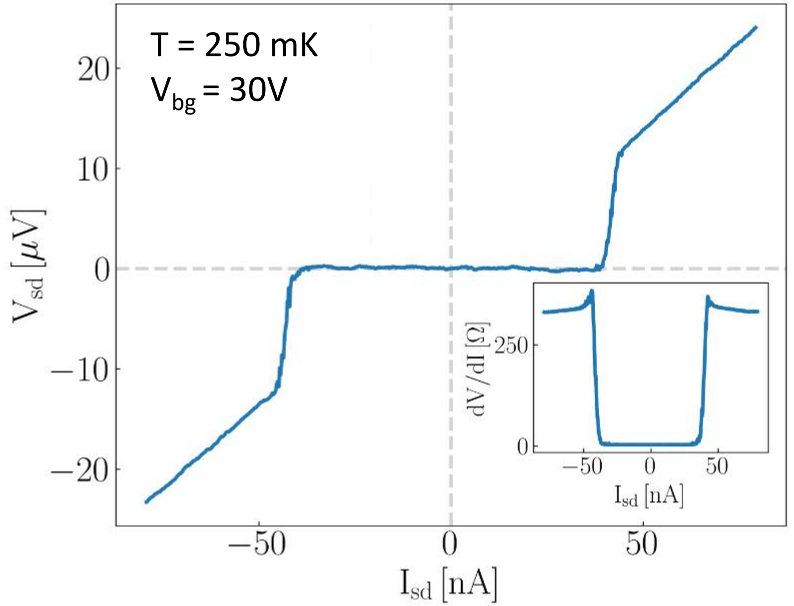

50 nA supercurrent

Gate tunable supercurrent

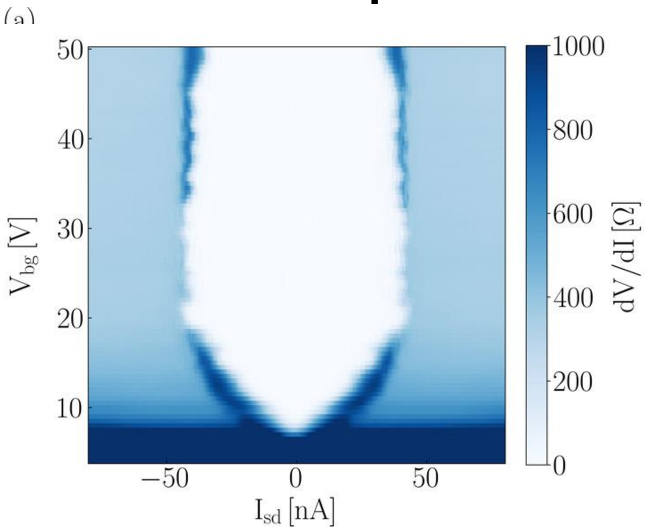

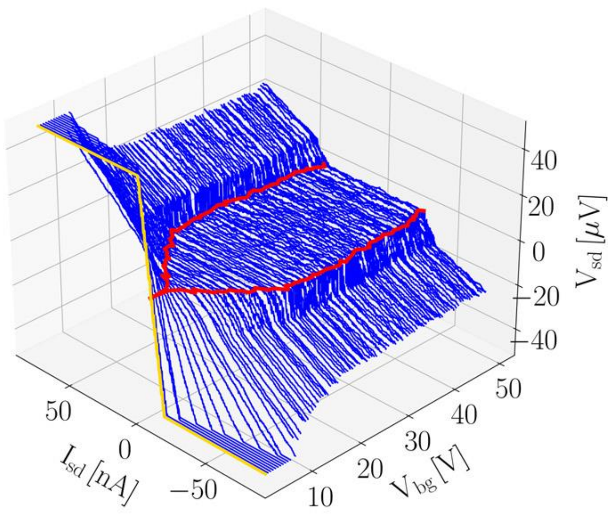

Color plot of the differential resistance

Further info:

S. Salimian et al. “Gate-controlled supercurrent in ballistic InSb nanoflag Josephson junctions” *Appl. Phys. Lett.*, 119, no. 21, 2021 doi: 10.1063/5.0071218

Conclusions

- Finding the parameters that affect axial and radial growth is important for controlling and tuning the nanostructure morphology

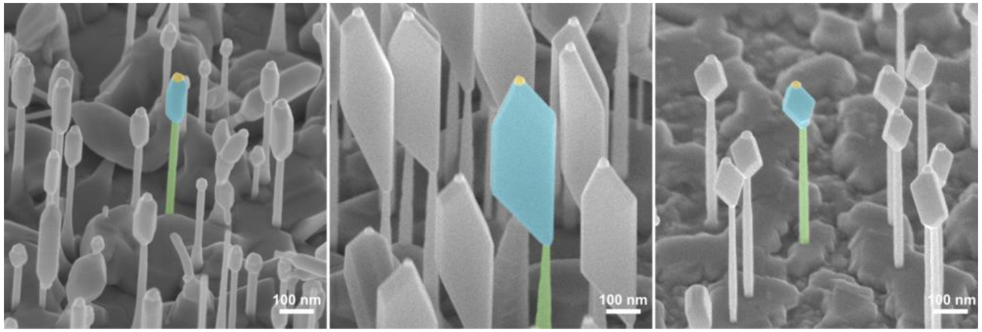

- Directional growth and more robust InP NW stems were employed to achieve large single-crystalline NFs

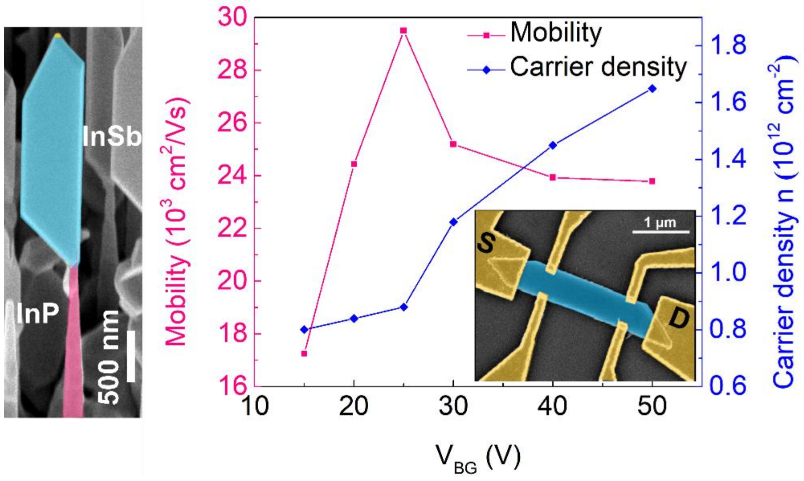

- A simplified growth model was developed, allowing for semi-quantitative description of the NF morphology evolution.
- Electron Hall mobility of about 29500 cm^2/Vs Mean free path upto 500 nm.

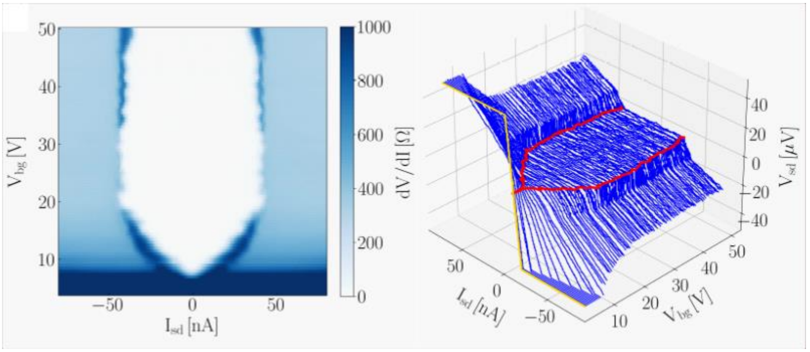

- NFs-based Josephson junction devices showed gate tunable supercurrent
- InSb NFs: versatile and convenient 2D platform for advanced quantum technologies.

Thanks to...

Isha Verma
Ph.D. student

e-mail: isha.verma@sns.it

Daniele Ercolani

Lucia Sorba

TEM Characterization

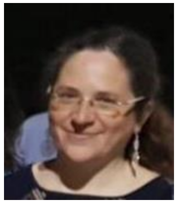

Francesca Rossi

Transport Measurements

Sedighe Salimian

Stefan Heun

Theoretical Modeling

Vladimir Dubrovskii

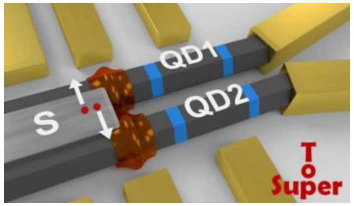

This research activity was partially supported by the **SUPERTOP** project, QUANTERA ERA-NET Cofound in Quantum Technologies (H2020 Grant No. 731473) and by the FET-OPEN project **AndQC** (H2020 Grant No. 828948).

AndQC

Thank you for your attention!